Orientation dependence of interlayer coupling and interlayer moments in Fe/Cr multilayers

M. A. Tomaz and W. J. Antel, Jr.
Department of Physics and Astronomy, Ohio University, Athens, Ohio 45701

W. L. O'Brien
Synchrotron Radiation Center, University of Wisconsin-Madison, 3731 Schneider Dr., Stoughton, Wisconsin 53589

G. R. Harp
Department of Physics and Astronomy, Ohio University, Athens, Ohio 45701
(Received 5 September 1996; revised manuscript received 15 October 1996)

The relationship between indirect exchange coupling and interlayer d-electron magnetic moments is studied using magnetometry and x-ray magnetic circular dichroism (XMCD) in Fe/Cr multilayers. Multilayers are simultaneously prepared with growth axes along different crystallographic orientations to determine the orientation dependence of these properties. We find the Cr moments are antiparallel to the Fe, and that a Cr thickness (t_{Cr}) of 1 ML has a moment of $\approx -0.7\mu_B$, 50% larger than the Cr moment developed in Fe-based dilute Cr alloys. For larger t_{Cr} the Cr moment decays very quickly with distance from the Fe interface, while the Fe moment remains bulklike at all Cr thicknesses. It is found that for $t_{Cr}<10$ Å there are slight differences in the indirect (oscillatory) exchange coupling between Fe layers depending on crystallographic orientation. Intuitively, one would also expect an orientation dependence to the induced Cr moments, but we find them to be orientation independent. The orientation independence of the Cr moments correlates well with the orientation independent coupling which has been previously observed for $t_{Cr}>10$ Å. [S0163-1829(97)01306-4]

I. INTRODUCTION

Advances in preparation techniques now allow the production of ferromagnetic and/or nonmagnetic superlattices comprising layers only a few atoms thick. This enables the very interesting possibility of inducing magnetic moments in materials not normally magnetic by placing them in close proximity to a ferromagnetic layer. These ''interlayer'' magnetic moments are ultimately responsible for the oscillatory exchange coupling which is often observed in these systems.[1] This occurs as follows: hybridization at the ferromagnetic and/or nonmagnetic interface induces a magnetic moment (net spin polarization) in the electrons belonging to the interlayer atoms. This spin polarization decays and oscillates in sign as one moves away from the interface. At the subsequent interface, the ferromagnetic layer interacts with the remnant of this spin polarization leading to a decaying and oscillating exchange coupling between the ferromagnetic layers. Another way in which interlayer moments may contribute to exchange coupling is as ''loose spins,'' which are important to one model[2] for biquadratic (90°) exchange coupling.[3]

Indirect exchange coupling is generally expected to be orientation dependent, since (in an RKKY model) it depends on the magnitude of the Fermi wave vector parallel to the growth axis.[4] This has been verified specifically in Fe/Cr through first-principles calculations of multilayers in various orientations.[5,6] Thus, a recent result which shows an orientation *independence* of the ''long'' period coupling in Fe/Cr (100) and (211) multilayers[7] is rather surprising. It is possible that the experimental result is caused by a coincidental equality of the coupling period for the two orientations.[8]

When calculated directly, the interlayer moments in Fe/Cr multilayers are predicted to depend on crystallographic orientation.[6] Additionally, their detailed behavior also depends on the nature of the Fe/Cr interface and the Fe moment configuration[9,8,6] (that is, whether the Fe layers are arranged ferromagnetically, antiferromagnetically, or otherwise).

For the (100) orientation, there is extensive literature on the magnetic ordering of Cr thin films deposited on the surface of Fe.[10–13] For nearly perfect Fe(100) substrates and high quality Fe/Cr interfaces, layer antiferromagnetism is observed in the Cr film,[10–12] which gives rise to ''short period'' antiferromagnetic coupling between Fe(100) films separated by Cr.[14] Imperfect interfaces, however, can suppress the Cr spin density wave[15] and the short period coupling[9] between Fe layers.

Much less work has focused on Cr moments in Fe/Cr multilayers, and orientation dependent measurements of moments in Fe/Cr have not been performed until now. These induced interlayer moments are crucial to our understanding of RKKY exchange coupling. The measurement of interlayer moments is challenging because the ferromagnetic layer moments overwhelm the very small interlayer moments. An element-specific probing technique is required. Here we apply x-ray magnetic circular dichroism (XMCD) to determine the layer-averaged values of the Fe and Cr moments in Fe/Cr multilayers both as a function of interlayer thickness and crystallographic orientation. Because XMCD is measured at the ''white line'' absorption features, it measures mainly the d-band component of the atomic magnetic moment. This allows us to probe the correlation between the d-band moments and the exchange coupling. But because the d-derived moments dominate the magnetic moments in transition metals, for convenience we shall simply refer to the XMCD results as measuring the atomic moments.

 © 1997 The American Physical Society

II. SAMPLE PREPARATION

The multilayers were prepared in a new sputter deposition system at Ohio University using established recipes.[7,16,17] This system has a base pressure of 1×10^{-9} Torr, and magnetron sputtering was performed at $\approx 3\times10^{-3}$ Torr. MgO(100), MgO(110), and Al_2O_3(1120) substrates were inserted together and initially heated to >550 °C for 20 min, followed by growth of the buffer layer (Cr 25 Å). The substrates were then allowed to cool to 100 °C ($\approx$ 4 h) at which time a multilayer with structure Fe 7.5 Å/[Cr t_{Cr}/Fe 7.5 Å $]_{40}$ was deposited, followed by a protective Al 20 Å capping layer. Here t_{Cr} = 1.5, 3, 4.5, 6, 7.5, 9, 12, 15, and 20 Å. Only multilayers with t_{Cr} = 1–20 Å were studied since, as shown below, the Cr atoms are most strongly polarized at the Fe interface, and the average Cr moment is maximized for thin Cr layers. The substrate holder was rotated at >1 Hz during deposition to ensure uniform thicknesses across the different substrates. It was found that with an Al 20 Å capping layer, no detectable oxidation of the Fe or Cr was evident in any of the films (as determined by x-ray absorption spectroscopy). Such oxidation was problematic in a previous study of Fe/V.[18]

III. STRUCTURAL CHARACTERIZATION

Following deposition, the samples were removed from vacuum and characterized by x-ray diffraction. The specular diffraction scans indicated a single vertical orientation corresponding to (100), (211), or (110) for films deposited on MgO(100), MgO(110), and Al_2O_3(1120), respectively. Representative x-ray scans are presented in Fig. 1 from the Fe/Cr 7.5 Å samples. Here we observe only those diffraction features associated with (100), (211), or (110) orientations of the respective Fe/Cr multilayers (i.e., no other orientations are present). Beside these scans, x-ray rocking curves through the strongest Fe/Cr features are presented for each of the films. We observed rocking curve full width at half maxima (FWHM) of $\approx$ 1° in the (100) and (211) oriented films. The (110) rocking curve FWHM were sometimes broader; the widest one was observed for the Fe/Cr(110) 15 Å multilayer and was over 2°.

IV. MAGNETOMETRY

The samples were characterized using the magneto-optical Kerr effect (MOKE) loops along various in-plane azimuthal orientations for each sample. From these loops, the easy and hard axes of each sample were determined. Although we could not determine which in-plane crystallographic direction is associated with the easy axis in each sample, it was possible to verify that each sample's anisotropy showed the symmetry corresponding to its epitaxial orientation. Thus the (100) samples showed a fourfold magnetic anisotropy (two easy-axes in-plane separated by 90°), while the (110) and (211) samples showed a twofold in-plane magnetic symmetry.

Representative MOKE loops are presented in Figs. 2–4. We observe that the difference between easy- and hard-axis loops is prominent only in samples having strong ferromagnetic coupling between Fe layers. Some samples, such as

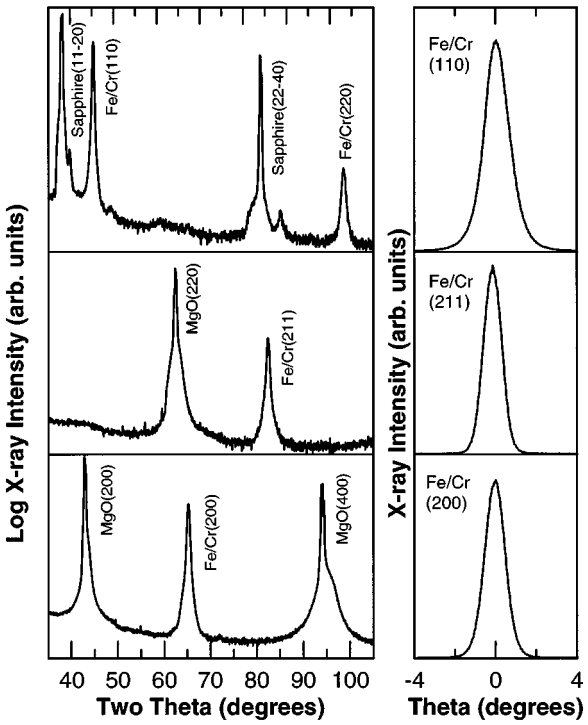

FIG. 1. Specular (left) x-ray diffraction scans from three Fe/Cr multilayers grown simultaneously on MgO(100) (lower), MgO(110) (middle) and Al_2O_3(1120) (upper) substrates with structure: Substrate/Cr 25 Å/Fe 7.5 Å/[Cr 7.5 Å/Fe 7.5 Å$]_{40}$/Al 20 Å. On each substrate only a single crystallographic orientation is observed, corresponding to the bcc(100), bcc(211), and bcc(110) growth axes, respectively. To the right of each specular scan, rocking curves through the strongest multilayer peak are displayed. Rocking curves typically have FWHM of $\approx$1°.

those with t_{Cr} = 12 Å showed low remanence and very high saturation fields independent of the azimuthal orientation. This is indicative of antiferromagnetic coupling between the Fe layers. Such AF coupling for Cr 12 Å layers agrees with previous results on Fe/Cr(100) and Fe/Cr(211) multilayers.[7]

From easy-axis loops such as those in Figs. 2–4, we determined the applied field required to bring each film to 80% of its saturation magnetization. This 80% saturation field is plotted in Fig. 5 for all of the samples. The filled data points were taken from loops that were not saturated even in the largest field applied in our instrument (8 kOe). Therefore, these data points represent lower limits for the 80% saturation field. We find that this saturation field exhibits a strong peak centered near t_{Cr} = 10 Å for every orientation of our Fe/Cr films, indicative of AF coupling.

However, the minimum Cr thickness where nonferromagnetic coupling occurs is different in each orientation. A dashed vertical line is drawn in the figure to highlight this feature. Nonferromagnetic coupling begins at t_{Cr} = 4.5 Å in Fe/Cr(110), 6 Å in Fe/Cr(100), and 7.5 Å in Fe/Cr(211). Because the three orientations were deposited *simultaneously*, there is no possibility that layer thickness variations are responsible for these differences.[19]

In Fig. 6, we present another method for visualizing the coupling. Here we plot the ratio M_{600}/M_{8000}: the magnetization of each sample in 600 Oe applied field divided by its

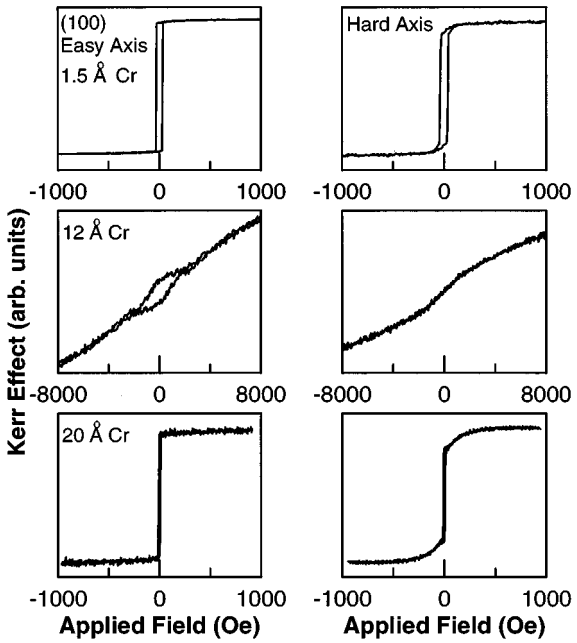

FIG. 2. Magnetization loops along the easy and hard axes of three Fe/Cr(100) multilayers having Cr layer thicknesses of 1.5, 12, and 20 Å. Very strong antiferromagnetic coupling is observed in the 12 Å film. At 1.5 and 20 Å, ferromagnetic coupling permits the observation of the in-plane anisotropy of the films. The easy and hard axes were related by a 45° in-plane rotation (fourfold).

magnetization in 8000 Oe. Filled symbols indicate which samples were not saturated in 8000 Oe. For the thinnest and thickest films, $M_{600}/M_{8000} \approx 1$, indicating the films were fully saturated in 600 Oe applied field. For t_{Cr} near 10 Å, M_{600}/M_{8000} is much smaller than 1, indicating AF coupling. Once again, the onset of nonferromagnetic coupling appears

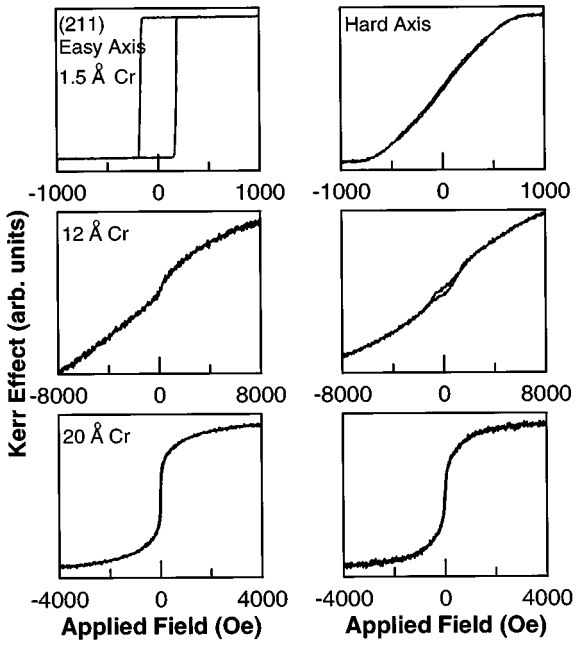

FIG. 3. As in Fig. 2, but for Fe/Cr(211) films. Here the in-plane anisotropy is twofold, and the easy and hard axes are related by a 90° in-plane rotation.

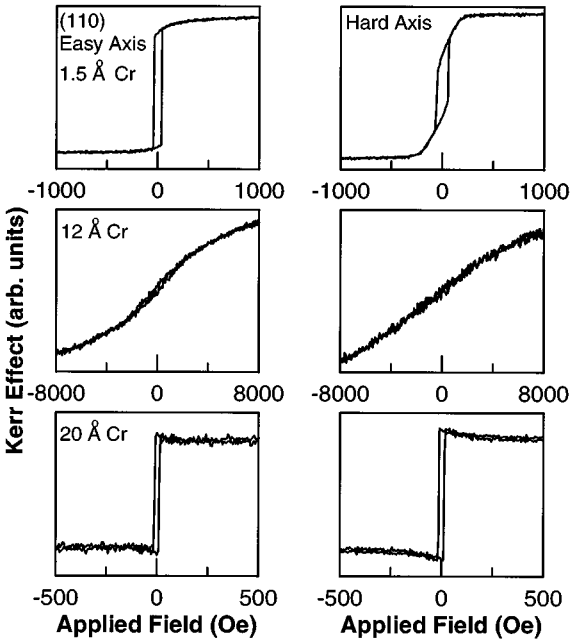

FIG. 4. As in Figs. 2 and 3, but for Fe/Cr(110) films. Here the in-plane anisotropy is again twofold, with easy and hard directions related by a 90° in-plane rotation.

to occur first in Fe/Cr(110), second in Fe/Cr(100), and last of all in Fe/Cr(211). We point out that the orientation dependence (OD) of the exchange coupling reported here is not inconsistent with the orientation *independent* coupling observed in Ref. 7 since the previous study focused mainly on multilayers with larger t_{Cr}.

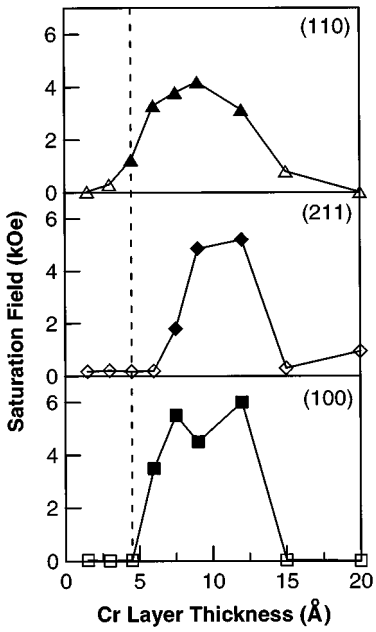

FIG. 5. Plot of the 80% saturation field for Fe/Cr (100), (211), and (110) multilayers as a function of t_{Cr}. Each orientation shows a peak near t_{Cr} = 10 Å, indicating antiferromagnetic coupling. The filled symbols indicate samples which could not be saturated in 8 kOe. The vertical dashed line highlights the result that there is an orientation dependence to the interlayer coupling in the low thickness regime.

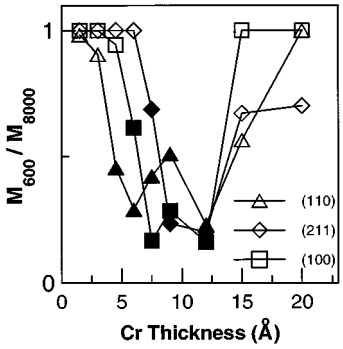

FIG. 6. Plot of the Kerr effect at 600 Oe divided by the Kerr effect at 8 kOe for all the films in this study. Filled symbols indicate films which were not saturated in 8 kOe. In this figure, it is even more evident that there is an orientation dependence to the onset of nonferromagnetic coupling in these films.

While we observe a definite OD to the coupling, one must keep in mind that this OD could be due either to intrinsic or extrinsic factors. Examples of extrinsic factors include OD of layer roughness, OD of Fe-Cr interdiffusion, etc. Indeed, Folkerts and Hakkens[20] found that Fe/Cr(110) superlattices spontaneously facet to present (100) and (010) faces, which have a lower surface energy. Presumably, similar faceting would not occur on the (100) orientation since there is no energy advantage. Such extrinsic factors could move the effective Fe/Cr interface relative to the nominal interface, making the Cr layers behave as if they were thinner or thicker as regards coupling. Another way roughness can affect coupling is through the enhancement of biquadratic coupling.[2] This might explain the large biquadratic coupling that has recently been observed in Fe/Cr(110) by Elmers *et al.*[21]

Whatever the cause of the OD of the interlayer coupling observed here, Fe/Cr presents a good system for the study of the OD of the induced interlayer moments. This is because the OD of the indirect exchange coupling occurs in an interlayer thickness range where we expect the strongest XMCD signal. In the following section, we discuss the measurement and results for the interlayer moments.

V. ELEMENT SPECIFIC MAGNETOMETRY

A. Determining magnetic moments

XMCD studies were performed at the Synchrotron Radiation Center on the 10M toroidal grating monochromator. This monochromator is equipped with a scanning vertical aperture which allows the selection of linearly (100%) or circularly ($\approx$ 85%) polarized radiation. XMCD measurements were made at the Fe and Cr 2*p* absorption edges using a new system which allows the application of 0–1.5 kOe fields in the sample plane. The photon beam was incident at an angle of 45° and the projection of the photon wave vector into the sample plane was either parallel or antiparallel to the applied field direction. The applied magnetic field was switched at each photon energy, and in this way two absorption spectra were obtained, $\alpha_r(\hbar\omega)$ and $\alpha_l(\hbar\omega)$. Samples were measured in remanence where possible, or in field when the remanent magnetization was low. The x-ray absorption spectra, obtained using a total yield technique, were normalized to the incident photon flux.

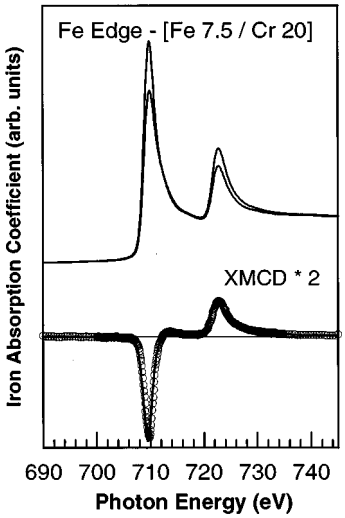

FIG. 7. Absorption spectra and XMCD (difference spectrum) at the Fe edge from an Fe/Cr(100) film with t_{Cr} = 20 Å. The XMCD data (circles) are compared with a scaled version of the XMCD from a standard sample (filled line). From the scaling factor of the filled line, the average Fe magnetic moment in the 20 Å film is determined.

We deduce the projected magnetic moment from the XMCD spectra in the following way. The spectra from all ''unknown'' samples are compared to a ''standard'' sample. The standard sample is chosen to be one for which we know the absolute magnetic moment by some other method. First, $\alpha_r(\hbar\omega)$ and $\alpha_l(\hbar\omega)$ of the standard and unknown are normalized to a per-atom basis. We then compare the XMCD, $\alpha_m=(\alpha_r-\alpha_l)$, of the unknown to that of the standard. More specifically, we determine the value of M which minimizes

$$\chi^2 \equiv \Sigma_i (\alpha^U_{m,i} - M\alpha^S_{m,i})^2, \tag{1}$$

where U and S denote the unknown and standard, and the sum on i is taken over all data points in the photon energy range near the absorption edge. M represents the projected average magnetic moment in the unknown multilayer in units of the standard moment. We also obtain an estimate of the *statistical* error bar in M by determining what variation of M is required to change χ^2 by 10% from its minimum value. (There is also a systematic error which is dominated by the magnetic dipole contribution to the XMCD and is of order 15% of M.[22]) The magnetic moments are then corrected (if necessary) using the MOKE loops so that they correspond to the moment at 600 Oe.

The above method for determining magnetic moments was developed especially for cases where the induced magnetic moment is small. Instead of just reporting the ''peak'' dichroism as is sometimes done, we compare dichroism signals over the entire spectrum. Statistically, this provides the best estimate of the magnetic moment.

As an example of this process, we display in Figs. 7 and 8 the absorption spectra and XMCD from an Fe/Cr(100) multilayer. We present data from a t_{Cr} = 20 Å sample to highlight the sensitivity of our measurements since this is the ''worst case,'' where the Cr dichroism signal is lowest as compared to its absorption coefficient. In the upper portion of these figures, we display α_r and α_l at the Fe and Cr

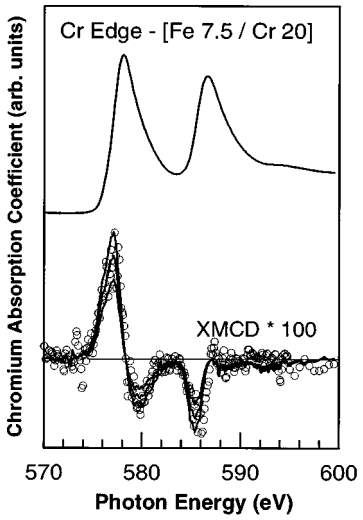

FIG. 8. As in Fig. 7, but at the Cr edge. Here the XMCD is much weaker due to the small induced moment on the Cr interlayers. Three scaled versions of the standard Cr spectrum are displayed, indicating the best fit and the upper and lower bound of our statistical error bar for the average magnetic moment of Cr atoms in this film (see text for details).

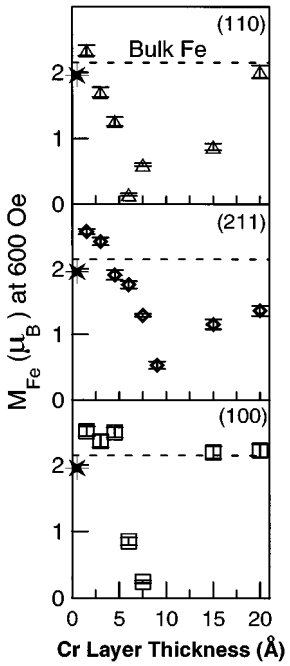

FIG. 9. Summary of the projected Fe moments in 600 Oe applied field as determined by XMCD. Statistical error bars are shown, although the systematic error bars may be larger (see Ref. 22). For comparison, all graphs display a dashed line at the bulk Fe moment and a starburst symbol representing data from an $Fe_{94}Cr_6$ alloy. These curves look strikingly similar to those of Fig. 6. This indicates that while the *net* Fe moment is often reduced by AF coupling, individual Fe layers possess bulklike moment magnitudes.

absorption edge, respectively. In the lower panel, α_m is displayed (circles). Superimposed on α_m are three scaled versions of the standard dichroism spectrum for that element. These three standard spectra correspond to the best fit, and the upper and lower limit of the error bar. In the Fe case, the fit is of such high quality that the separate standard dichroism spectra are indistinguishable.

B. Element-specific magnetic moments

Figure 9 displays the XMCD results for the projected Fe moments. The Fe spectra were compared to an Fe 250 Å thick film deposited on MgO(110) with the usual Al capping layer, for which we assume a moment of $\approx 2.2\mu_B$. It is seen that for thin interlayers the Fe magnetic moment is close to or slightly enhanced over that of bulk Fe. For larger Cr thickness, the projected Fe moment falls due to the onset of nonferromagnetic coupling. XMCD measurements were not performed for most of the $t_{Cr}=$ 9 and 12 Å samples since the antiferromagnetic coupling was so strong as to preclude meaningful measurements.

The Fe curves look very similar to those of Fig. 6. This is expected, since the Fe moments dominate the MOKE signal in Fig. 6. But the similarity of Figs. 6 and 9 provides one important piece of information: it indicates that the Fe atomic moments deviate little from the bulk value in any of these films. This result agrees well with previous calculations where the interface Fe moments are slightly suppressed and the interior Fe layers are slightly enhanced giving little net change in the average Fe moment from its bulk value.[6]

Moving to the Cr moments, Cr XMCD spectra were compared to the ''standard'' spectrum of an $Fe_{94}Cr_6$ alloy where previous studies[23,24] indicate a magnetic moment of $-0.4\pm0.4\mu_B$. Because of the large error bars in the previous studies, we made an independent determination of the alloy moment using a ''transfer'' of the XMCD proportionality constants[28] from Fe and from V, which nicely bracket Cr (in the Periodic Table). The constants for Fe were found above, and those for V were determined from an $Fe_{94}V_6$ alloy, where previous hyperfine field[23] and neutron diffraction[24] studies indicate a V magnetic moment of $-0.3\pm0.2\mu_B$ (averaging the results from the two publications). This analysis concluded that the alloy Cr moment was $\approx -0.4\mu_B$ (using Fe coefficients) and $\approx -0.6\mu_B$ (using V coefficients). As a compromise, we assigned an average value of $-0.47\mu_B$ to the alloy Cr moment.

In the multilayers, we found that the layer averaged Cr atomic moments were always aligned antiparallel to the Fe, as shown in Fig. 10. Note that we plot the negative of the Cr moment. Remarkably, the induced Cr moment is higher in the 1.5 Å Cr layers than in the $Fe_{94}Cr_6$ alloy. The alloy is indicated with a starburst at the horizontal position corresponding to a multilayer with the same composition. Alloys with more Cr are expected to show even lower Cr moments. This is compared with the $t_{Cr}=1.5$ Å multilayer which has an average composition of $Fe_{84}Cr_{16}$. This result is independent of the exact vertical scale since it comes from a direct comparison of the XMCD from the multilayers and the alloy. We conclude that layering Cr with Fe is more effective at inducing interlayer moments than alloying Cr with Fe, for a given average composition. This is in agreement with previous theoretical studies (see, e.g., Ref. 6).

VI. DISCUSSION

In the multilayers, the magnitude of the Cr moments follows a pattern which is a product of the projected Fe moment

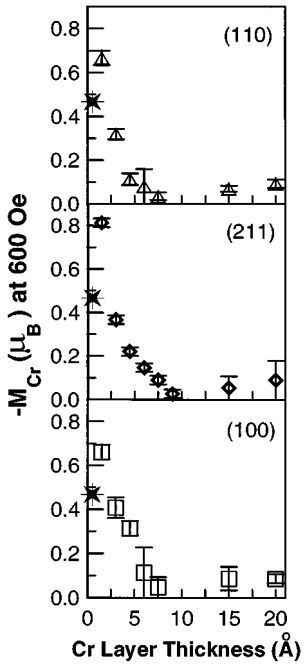

FIG. 10. Similar to Fig. 9 but displaying Cr moments. We observe that the Cr moments follow the trend of the Fe moments, but with an additional decaying factor with increasing t_{Cr}. Remarkably, the Cr moments developed in multilayers with $t_{Cr}=1.5$ Å (average composition $Fe_{84}Cr_{16}$) are larger than is developed in the $Fe_{94}Cr_6$ alloy (see text).

times a function which decays with increasing t_{Cr}. The dependence on the Fe moment is expected since in the absence of Fe, the Cr would be paramagnetic.[25] To remove this trivial dependence of the Cr moment on the projected Fe moment, we define the ''interlayer susceptibility,'' X_{Cr}, defined as[26]

$$X_{Cr}=\frac{M_{Cr}}{M_{Fe}}. \tag{2}$$

X_{Cr} is plotted in Fig. 11.

Figure 11 shows that X_{Cr} does *not* depend on crystallographic orientation. This is somewhat surprising since the coupling is orientation dependent and is thought to be *mediated* by the interlayer moments.[4] Moreover, this does not agree with the results of recent calculations which predict an OD of the induced Cr moments.[6] Yet in all cases X_{Cr} is the same for the three crystallographic orientations to within experimental error.

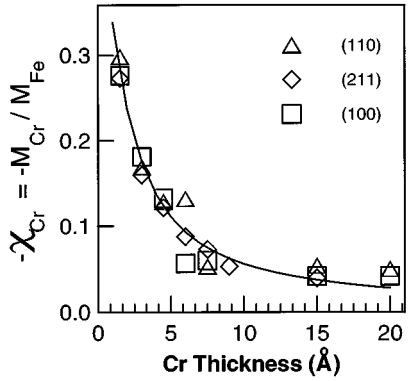

FIG. 11. The Cr interlayer susceptibilities, X_{Cr} for all the films. Surprisingly, X_{Cr} falls on a universal curve independent of crystallographic orientation. This is distinct from the predictions of previous calculations. The solid line is the fit of a model described in the text.

X_{Cr} decays with increasing t_{Cr} in a manner reminiscent of a dilution effect, or $1/t_{Cr}$ dependence. We conclude that only Cr atoms close to the Fe interface acquire a significant magnetic moment, and that the moments of atoms in the layer interior are negligible. This decay is quantified with a simple model. Suppose that a Cr atom at position z is exchange coupled to the adjacent Fe layers with a strength that decays exponentially with distance from the Fe layer:

$$\mathbf{M}_{Cr}(z)=\frac{A}{2\lambda_{Cr}}\{\mathbf{M}_1\exp(-z/\lambda_{Cr})+\mathbf{M}_2\exp[-(t_{Cr}-z)/\lambda_{Cr}]\}, \tag{3}$$

where $\mathbf{M}_1$ and $\mathbf{M}_2$ are the vector magnetizations of the Fe layers located at $z=0$ and $z=t_{Cr}$, respectively, and A and λ_{Cr} are arbitrary constants. In the case of nonferromagnetic coupling, we assume that both Fe layers are aligned symmetrically about the applied field direction.

To obtain the average Cr moment, $\mathbf{M}_{Cr}(z)$ is projected onto the measurement direction and then integrated over the thickness of the layer. Finally we divide by t_{Cr} to obtain the average Cr moment per atom,

$$M_{Cr}^{ave}=A\frac{M_{Fe}[1-\exp(-t_{Cr}/\lambda_{Cr})]}{t_{Cr}}, \tag{4}$$

where M_{Fe} is the projected Fe moment of either of the Fe layers. We divide by M_{Fe}, and obtain an expression that can be compared with X_{Cr}, and this is done in Fig. 11 (solid line).

Besides its evident simplicity, this model was chosen because it has the correct asymptotic behavior: M_{Cr}^{ave} is finite as $t_{Cr}\to 0$, and it decays as $1/t_{Cr}$ for large t_{Cr}. In Fig. 11, the parameters A and λ_{Cr} have been adjusted to obtain the best fit. The model simulates the data well, and allows us to extract the exchange coupling decay length, $\lambda_{Cr}=1.1$ Å.

To help visualize Eq. (4), we plot in Fig. 12 the model results for Cr moments in Fe/Cr(100) multilayers having 1, 3, 5, and 7 monolayers of Cr. Along other orientations, the results would be qualitatively the same, but with somewhat different moment values in each layer (due to the different thicknesses associated with a monolayer along each direction). In each case, the Cr layers are assumed to be bracketed by ferromagnetically aligned Fe layers with moments of 2.2 μ_B. Note that the Cr moments decay rapidly toward the interior of the layer. Beyond 7 ML, thicker Cr only results in the addition of nonmagnetic Cr layers to the center of the Cr layer. The interface Cr atoms always have about the same moment ($\approx -0.35\mu_B$) except for 1 or 2 ML thicknesses (approximately 1.5 or 3 Å) where the interface Cr atoms acquire a larger moment (up to $-0.7\mu_B$ for 1 ML Cr).

It is instructive to compare the Cr moment magnitudes with those obtained for Cr films on Fe(100). One direct comparison can be made to the work of Idzerda *et al.*,[13] who also used XMCD as a probe. For 0.25 ML Cr on Fe they saw an XMCD to absorption peak ratio of 7.2% for Cr. Using a

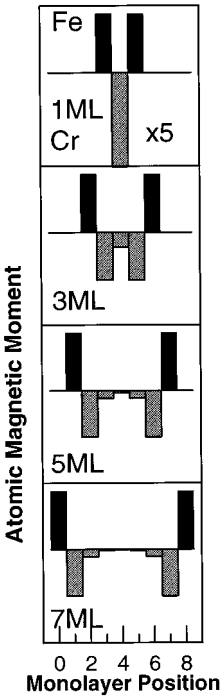

FIG. 12. The Cr moments as a function of t_{Cr} for Fe/Cr(100) as deduced from the fit of Fig. 11. The Cr moments (crosshatched bars) have been multiplied by 5 in order to bring out their detail in the presence of the Fe moments (filled bars).

different standardization method to that used here, they arrived at a Cr moment of $-0.6\pm0.2\mu_B$ for this film. This is comparable to our observation of a 7.7% XMCD to absorption ratio for 1 ML Cr sandwiched between Fe (after correcting for the finite angle of incidence and incomplete circular polarization), for which we arrive at a Cr moment of $-0.7\mu_B$. The excellent agreement of XMCD to magnetic moment scaling factors in these two studies lends credibility to both of them.

Idzerda *et al.*[13] find a rapid decay of the Cr moment with increasing Cr layer thickness, with the moment dropping to $\approx -0.2\mu_B$ for a 1 ML Cr film. In contrast, Turtur and Bayreuther[12] find that the first two Cr monolayers have a constant Cr moment of $\approx -3\mu_B$. The differences between the two studies may have to do with sample preparation. It is difficult to compare Cr thin films which have one Fe interface to Cr in multilayers with two Fe interfaces. However, doing so suggests that the present study is qualitatively more similar to the study of Idzerda.

In the present work, the localization of the induced Cr moment to the interface is evidence for frustration of the interior Cr moments by (1) interface roughness and (2) the fact that we force the Fe layers into ferromagnetic alignment for XMCD measurements, even when the ground state is an antiferromagnetic configuration. Both of these factors are known to suppress layer antiferromagnetism, short period exchange coupling, and the magnitude of Cr magnetic moments in Fe/Cr multilayers. These issues have been discussed in Refs. 9, 15, and 6. Note that Eq. (4) neglects the effects of roughness in these films. Because we have no information quantifying the roughness, we have chosen to ignore it in our analysis. We point out, however, that such roughness must be limited, since certain multilayer effects survive, including the long period exchange coupling.

Another multilayer effect is the enhancement of the induced Cr moments for multilayers above those observed in alloys with similar composition. This is in agreement with a previous theoretical study.[6] One way of understanding this is that in a multilayer, the Cr atoms are segregated from the Fe atoms and thus interfere less with the Fe magnetic moments. It is known that in alloys with greater Cr concentration, the Fe moments are suppressed.[27] Likewise, Cr atom segregation may reduce Fe interference in the development of the Cr moments. Both of these effects are likely to lead to higher induced Cr moments for multilayers as compared with alloys.

The OD of the indirect exchange coupling is not reflected in the interlayer moments. An assumption that the exchange coupling is intrinsically orientation dependent would indicate that the d-band moments are not the dominant mediators of long-period coupling for $t_{Cr}<10$ Å. In this case, the sp-derived bands would appear to dominate the coupling. Even though the sp moments are small (and not measurable in the present experiment), they can dominate the coupling in Mo(100) and Nb(100) spacer layers as was pointed out by Koelling.[8] Ironically, in the same article Koelling concludes that the long coupling period in Fe/Cr(100) could only be due to d-band electron states.

The simplest resolution of this dilemma is to suppose that the OD of the indirect exchange coupling is caused by an OD of extrinsic factors such as interface roughness. Another possibility is that while the sp bands are important to coupling for small t_{Cr}, the sp-band effects become weak for $t_{Cr}>10$ Å. This kind of behavior has been seen in recent calculations of Co/Cu multilayers by Samant *et al.*,[28] who report that the sp-band moments decay much more quickly away from the interface than do the d-band moments.

For greater Cr layer thicknesses, the exchange coupling is orientation independent, at least for the (100) and (211) orientations as shown by Fullerton *et al.*[7] This is in good agreement with the orientation independence of the d-band interlayer moments observed here. This also supports the conclusion of Koelling[8] that the long period coupling is dependent on d-derived states. In that article, Koelling argues that the d-band ''lens'' of the Cr Fermi surface gives rise to the long period coupling, and that the shape of this lens is such that the long coupling period is the same along (100), (211), and (110) orientations.

VII. CONCLUSIONS

Our results show that there is a slight orientation dependence to the long period exchange coupling in Fe/Cr in the low thickness regime. In the same films, however, the interlayer moments are identical to within experimental error across three different growth orientations: (100), (211), and (110). The induced Cr moments are antiparallel to the Fe moments, and for interlayers 1 ML thick, have a magnitude of about $-0.7\mu_B$ per atom. By direct comparison, we observe that these multilayers have 1.5 times the Cr moment developed in dilute Cr-Fe alloys, establishing that the multilayer geometry is more effective at inducing interlayer moments in Cr than the alloy geometry.

The thickness dependence of the Cr moments agrees with a model assuming an exponential decay of the moment as a function of distance from the Fe interface, with a decay constant of 1.1 Å. The Fe atomic moments remain close to that of bulk Fe. The orientation independence of the *d*-derived moments observed here correlates well with the orientation independence of the interlayer exchange coupling for $t_{Cr} > 10$ Å which was observed in a previous study.[7] This relationship between *d* moments and interlayer coupling suggests that the long period coupling in Fe/Cr is mediated by *d*-derived electron states, as was suggested by calculations.[8]

ACKNOWLEDGMENTS

The authors gratefully acknowledge the support of the Ohio University Research Council and the National Science Foundation under CAREER Award No. DMR-9623246. The Synchrotron Radiation Center was supported by the National Science Foundation under Award No. DMR-9212658.

[1] S. S. P. Parkin, N. More, and K. P. Roche, Phys. Rev. Lett. **64**, 2304 (1990).

[2] J. C. Slonczewski, J. Appl. Phys. **73**, 5957 (1993).

[3] M. Rührig, R. Schäfer, A. Hubert, R. Mosler, J. A. Wolf, S. Demokritov, and P. Grünberg, Phys. Status Solidi A **125**, 635 (1991).

[4] For a recent review of the theory of exchange coupling see K. B. Hathaway, in *Ultrathin Magnetic Structures II*, edited by B. Heinrich and J. A. C. Bland (Springer-Verlag, Berlin, 1994), p. 45.

[5] M. van Schilfgaarde, F. Herman, S. S. P. Parkin, and J. Kudrnovsky, Phys. Rev. Lett. **74**, 4063 (1995).

[6] R. Coehoorn, J. Magn. Magn. Mater. **151**, 341 (1995).

[7] E. E. Fullerton, M. J. Conover, J. E. Mattson, C. H. Sowers, and S. D. Bader, Phys. Rev. B **48**, 15 755 (1993).

[8] D. D. Koelling, Phys. Rev. B **50**, 273 (1994).

[9] D. Stoeffler and F. Gautier, Phys. Rev. B **44**, 10 389 (1991).

[10] T. G. Walker, A. W. Pang, H. Hopster, and S. F. Alvarado, Phys. Rev. Lett. **69**, 1121 (1992).

[11] D. T. Pierce, R. J. Celotta, and J. Unguris, J. Appl. Phys. **73**, 6201 (1993).

[12] C. Turtur and G. Bayreuther, Phys. Rev. Lett. **72**, 1557 (1994).

[13] Y. U. Idzerda, L. H. Tjeng, H.-J. Lin, C. J. Gutierrez, G. Meigs, and C. T. Chen, Phys. Rev. B **48**, 4144 (1993).

[14] J. Unguris, R. J. Celotta, and D. T. Pierce, Phys. Rev. Lett. **69**, 1125 (1992).

[15] E. E. Fullerton, K. T. Riggs, C. H. Sowers, S. D. Bader, and A. Berger, Phys. Rev. Lett. **75**, 330 (1995).

[16] G. R. Harp and S. S. P. Parkin, Appl. Phys. Lett. **65**, 3063 (1994).

[17] G. R. Harp and S. S. P. Parkin, Thin Solid Films (to be published).

[18] G. R. Harp, S. S. P. Parkin, W. L. O'Brien, and B. P. Tonner, Phys. Rev. B **51**, 3293 (1995).

[19] While the layer thicknesses for simultaneously deposited samples is the same, these thicknesses do not correspond to the equal numbers of monolayers in different orientations. Interestingly, the (110) orientation, which shows AF coupling at the smallest thickness, has the largest spacing between monolayers (2.03 Å). Conversely, coupling occurs last of all along the (211) orientation where the layer spacing is smallest (1.17 Å).

[20] W. Folkerts and F. Hakkens, J. Appl. Phys. **73**, 3922 (1993).

[21] H. J. Elmers, G. Liu, H. Fritzsche, and U. Gradmann, Phys. Rev. B **52**, R696 (1995).

[22] This method implicitly assumes that the shape of the dichroism signal is independent of the sample composition and/or orientation. To estimate what systematic error this assumption will introduce, consider that the dichroism signal consists of three parts: the spin moment, the orbital moment, and the magnetic dipole correction term. The sum of the orbital and spin moments is the total moment, while the magnetic dipole term is extraneous, i.e., noise. Over the past few years, powerful dichroism ''sum rules'' have been developed which in the most favorable circumstances permit independent determination of each of these quantities (Refs. 29–32). In recent measurements of Co/Au multilayers (Ref. 32) it was found that as a function of Au thickness, the orbital contribution to the Co moment changed by as much as $0.05\mu_B$ (in-plane geometry) and the magnetic dipole correction was as large as $0.11\mu_B$. These are to be compared to the dominant Co spin moment of $1.64\mu_B$ (total error of 10%). If this system can be taken as exemplary, our method for determining magnetic moments has a systematic error bar of 10%, or at worst, 20% of the total moment.

[23] M. B. Stearns and L. A. Feldkamp, Phys. Rev. B **13**, 1198 (1976).

[24] M. F. Collins and G. G. Low, Proc. Phys. Soc. London **86**, 458 (1965).

[25] Due to frustration caused by interface roughness in sputtered films such as these, the antiferromagnetic state of the Cr layers is suppressed for $t_{Cr} < \approx 40$ Å (Ref. 15).

[26] This is defined in analogy with the ordinary paramagnetic susceptibility, $M_{Cr}/H_{applied}$, by replacing $H_{applied}$ with H_{ex}, the exchange field due to the nearby Fe layer. In the simplest model, $H_{ex} \propto M_{Fe}$, hence our definition.

[27] M. V. Nevitt, and A. T. Aldred, J. Appl. Phys. **34**, 463 (1963).

[28] M. G. Samant, J. Stöhr, S. S. P. Parkin, G. A. Held, B. D. Hermsmeier, F. Herman, M. van Schilfgaarde, L.-C. Duda, D. C. Mancini, N. Wassdahl, and R. Nakajima, Phys. Rev. Lett. **72**, 1112 (1994).

[29] P. Carra, B. T. Thole, M. Altarelli, and X. Wang, Phys. Rev. Lett. **70**, 694 (1993).

[30] B. T. Thole, P. Carra, F. Sette, and G. van der Laan, Phys. Rev. Lett. **68**, 1943 (1992).

[31] J. Stöhr and H. König, Phys. Rev. Lett. **75**, 3748 (1995).

[32] D. Weller, J. Stöhr, R. Nakajima, A. Carl, M. G. Samant, C. Chappert, R. Megy, P. Beauvillain, P. Veillet, and G. A. Held, Phys. Rev. Lett. **75**, 3752 (1995).